


Article

# Critical Analysis of Process Integration Options for Joule-Cycle and Conventional Heat Pumps

Limei Gai <sup>1,\*</sup>, Petar Sabev Varbanov <sup>1</sup>, Timothy Gordon Walmsley <sup>2</sup> and Jiří Jaromír Klemes <sup>1</sup>

<sup>1</sup> Sustainable Process Integration Laboratory-SPIL, NETME Centre, Faculty of Mechanical Engineering, Brno University of Technology-VUT Brno, Technická 2896/2, 61600 Brno, Czech Republic; varbanov@fme.vutbr.cz (P.S.V.); klemes@fme.vutbr.cz (J.J.K.)

<sup>2</sup> Sustainable Energy and Water Systems Group, School of Engineering, The University of Waikato, Hamilton 3216, New Zealand; tim.walmsley@waikato.ac.nz

\* Correspondence: gai@fme.vutbr.cz

Received: 27 December 2019; Accepted: 26 January 2020; Published: 3 February 2020



**Abstract:** To date, research on heat pumps (HP) has mainly focused on vapour compression heat pumps (VCHP), transcritical heat pumps (TCHP), absorption heat pumps, and their heat integration with processes. Few studies have considered the Joule cycle heat pump (JCHP), which raises several questions. What are the characteristics and specifics of these different heat pumps? How are they different when they integrate with the processes? For different processes, which heat pump is more appropriate? To address these questions, the performance and integration of different types of heat pumps with various processes have been studied through Pinch Methodology. The results show that different heat pumps have their own optimal application range. The new JCHP is suitable for processes in which the temperature changes of source and sink are both massive. The VCHP is more suitable for the source and sink temperatures, which are near-constant. The TCHP is more suitable for sources with small temperature changes and sinks with large temperature changes. This study develops an approach that provides guidance for the selection of heat pumps by applying Process Integration to various combinations of heat pump types and processes. It is shown that the correct choice of heat pump type for each application is of utmost importance, as the Coefficient of Performance can be improved by up to an order of magnitude. By recovering and upgrading process waste heat, heat pumps can save 15–78% of the hot utility depending on the specific process.

**Keywords:** Process Integration; heat pumps; Joule cycle heat pump; Pinch Analysis

## 1. Introduction

### 1.1. Background

In the 21st century, energy crises, global warming and environmental pollution are becoming more and more serious. It is urgent to improve energy efficiency, save energy and reduce emissions. One of the critical issues is to valorise low potential waste heat instead of rejecting it. Appropriate integration of heat pumps has the characteristics of efficient recovery of low-temperature heat energy, hot utility energy-saving and potentially environmental protection. Heat pumps (HP) continue to receive considerable attention and development and are becoming a critical sustainable energy technology.

Sadi Carnot [1], a French scientist in the early 19th century, first proposed the “Carnot Cycle” theory in his paper in 1824, which became the origin of HP technology. In 1912, the world’s first set of HP equipment was successfully installed in Zurich, Switzerland with river water as the low heat source for heating. HPs entered the early stage of development from the 1940s to the early 1950s. HPs used in household, and industrial buildings began to enter the market. Since the 1970s,

the HP industry has advanced rapidly, and all countries have attached great importance to HP research. Large HP development plans have been instituted by countries and organisations such as the European Community and the International Energy Agency. At present, Europe, America and Japan are competing to develop new types of HPs.

### 1.2. State of the Art Review

Traditional HP technologies include the vapour compression heat pump (VCHP) [2], absorption heat pump [3], and transcritical heat pump [4]. Pavlas et al. [5] developed a Process Integration methodology for an HP integrated with a biomass gasification process of a wood processing plant. Liew and Walmsley [6] adopted a Total Site targeting method to integrate open cycle VCHP for enhancing overall site energy efficiency. Walmsley [7] presented a Total Site Heat Integration (TSHI) method for integrated evaporation systems using a HP (vapour recompression) effectively with application to milk concentrating. Walmsley et al. [8] performed a Pinch Analysis of hybrid compression–absorption HP process for convective dryers by employing to simulation and optimisation tools. Stampfli et al. [9] adapted Pinch Analysis to integrating VCHP for HPs in batch processes. A hybrid method [10] that unifies the insight-based and mathematical programming approaches has been proposed for industrial HP integration in batch processes to avoid long computation times. Another criterion EPC (i.e., the coefficient of performance in exergy per total annual cost) was proposed [11] for selecting HPs, modelling diverse types of HPs for operating conditions. This criterion can both evaluate the thermodynamic and economic performances of HPs.

Urbanucci et al. [12] proposed a two-level optimisation algorithm for the high-temperature HP integration in a trigeneration system. The proposed model allowed them to analyse the HP performance for various working fluids and operating conditions. Schlosser et al. [13] developed a model for evaluation of the efficiency gains of combining HP storage and intelligent system control for integrating multiple heat sources and sinks, reporting a significant reduction in energy demand. To integrate heat-upgrading technologies in process sites, Oluleye et al. [14] developed a systems-oriented criterion for conceptual screening and selection of HPs. A Mixed Integer Linear Programming (MILP) framework has been developed [15]. The screening criterion measured the exergy degradation of technology options. However, the techniques presented in that work are only applicable to conceptual system design. Goumba et al. [16] considered the different waste heat sources and proposed the “Recov’Heat” tool, for minimising the utility demands, which makes the heat pumping task easier.

The above studies only use known models to consider the integration of VCHP and processes. Some of the older HP types used Freon as a working fluid. However, Freon is no longer used because of its negative impact on the Earth’s atmospheric ozone [17]. In addition to the improvement the Coefficient of Performance (COP) of HPs and effective utilisation of the energy input, to further improve the environmental protection, engineers are committed to the development of new working fluids and HP technologies. HP applications are also in continuous development, is widely used in air conditioning and industrial fields and playing a significant role in terms of energy-saving and environmental protection.

Another type of HP with a commercial application is the TCHP, which uses CO<sub>2</sub> as a working fluid. CO<sub>2</sub> is a natural refrigerant, commonly known under the label “R744”. It has a relatively low global warming potential (GWP) value of only 1 and does not cause damage to the ozone layer. It is non-toxic, non-flammable, low-cost and easy to obtain. At present, hot water systems with CO<sub>2</sub> HPs usually adopt a transcritical cycle. In the early 1990s, Lorentzen [4] proposed a transcritical CO<sub>2</sub> cycle based on the specific physical properties of CO<sub>2</sub>, which significantly promoted the development of CO<sub>2</sub> systems in the field of refrigeration. Over the past twenty years, research institutions and enterprises in many countries around the world have done a lot of research on TCHP, which has become a research hotspot in the field of refrigeration. The exothermic process of significant temperature change (~80–100 °C) on the high-pressure side of the transcritical CO<sub>2</sub> system is very suitable for hot water heating. As a result, research on transcritical CO<sub>2</sub> HPs (TCHP) started as a hot water heater. Neksa et al. [18] built a test

device for a hot water HP system. The first demonstration TCHP water heater [19] was established for industrial use. Kim et al. [20] used a combined scroll expander–compressor unit in a two-stage compression CO<sub>2</sub> transcritical cycle to improve the cycle COP. Van de Bor et al. [21] compared several heat recovery technologies based on HPs and heat engines. Integration schemes with processes are not considered.

In VCHP and TCHP, the working fluid undergoes a phase change in at least one of the constituent processes, during which it absorbs or releases heat from the heat source to the heat exchanger (HX). This dependence on latent heat transfer may be a problem in some applications where average temperature variation is significant, exergy transfer efficiency is low, and COP is low. Fu and Gundersen [22] developed a HP for industrial applications based on the Joule cycle (which they called a reversed Brayton cycle). The operating parameters are investigated by thermodynamic and mathematical models, applying Pinch Analysis and Appropriate Placement rules. The provided case studies also illustrate the Heat Exchanger Network (HEN) synthesis conforming to the Heat Integration targets.

ECOP (Ecop Technologies GmbH) [23] applied a HP process based on a reverse Joule cycle (also known as Joule–Brayton or Brayton cycle) with the rotation HP implementation. Compared with the traditional HP, the Joule cycle heat pump (JCHP) features sensible heat exchange between the working fluid and process heat source/sink, which is an advantage when the process streams do not condense or evaporate or have smaller Specific Heat Capacity (CP). This provides more flexibility in accommodating process streams and achieving a higher temperature lift.

A recent work [24] has presented a system synthesis method for HP integration in the industry. The method uses a superstructure-based mathematical model, resulting in a Mixed Integer Nonlinear Programming (MINLP) formulation, achieving performance improvements over similar previous methods of up to 30%. The model considers phase-change based HPs (mainly VCHP). As is shown in this paper, the correct choice of HP type bears the significance of an order of magnitude higher than such improvements.

Many processes need heat transfer in industrial processing and power generation. Some need heating, and some need cooling or condensation. If the heat exchange network can be appropriately designed, the utility can be minimised, and the capital investment can be reduced to achieve energy saving. Pinch Analysis, pioneered by Linnhoff and Hindmarsh [25], has become a widely used method for the comprehensive design of heat exchange networks. The heat exchange network with minimum energy consumption can be obtained by optimising the heat recovery system, energy supply and process operation. Energy targeting is a powerful aid to process design and integration. Stampfli et al. [9] suggested the COP equation/curve for Process Integration with VCHP. According to the COP equation, when the condensation duty provided by the process sink is known, the evaporative duty of the HP can be obtained, and the COP curve can be drawn in Grand Composite Curve (GCC). The condensation duty can also be obtained when the process is used as a source. Gai et al. [26] extended the COP curve when the process was integrated with the JCHP. However, the COP curve for the Process Integration with a HP is derived under some assumptions or ideal conditions. Also, in the TCHP, the working fluid CO<sub>2</sub> is a transcritical cycle and the physical property changes substantially, so it is difficult to express the COP curve with an equation accurately.

### 1.3. Contributions and Novelty of This Study

A JCHP is more likely to obtain higher COP than a traditional HP under certain circumstances. However, there have been so far just a few studies on the use of JCHP and industrial processes. There is also a gap in the literature for a comparative analysis of different HP types, including the emerging JCHP. The COP equations of HP have some ideal assumptions. These results are in some deviation from the actual performance of the HP, which cannot well represent the real performance of the HP.

This study simulates and optimises the operation of the main classes of HPs in a process simulation software—Petro-SIM [27]—to get the performance of the HP, as much close to the reality as possible. These classes include the VCHP, TCHP and the JCHP.

The setting of various parameters considers possible process configurations. All COP curves and heat duties in the GCC for process and HP integration will be plotted against the actual data calculated in Petro-SIM. The choice of HP type should be performed based on the temperature–enthalpy profile of the considered industrial process for obtaining optimal performance. In this paper, the performance and application scope of three different HP systems—JCHP, VCHP, and TCHP—are discussed and compared to understand the energy-saving potential of applying the HP.

Section 2 introduces the simulation and optimisation of the considered HP types and the method of integration with the process for achieving heat recover. In Section 3, the suitability of the HP types to different temperature–enthalpy (T–H) profiles is evaluated, aiming at the minimisation of power consumption. The optimal COP of each integration case was obtained by optimising the operating parameters of the HP when given source and sink at different temperatures. In Section 4, the model is further applied to the integration of HP and different industrial process cases using Pinch Analysis, and the energy-saving potential of different types of HP is evaluated using the GCC [28].

## 2. Method

The main goal of heat pumping is to serve, simultaneously, part (or all) of the process heating and cooling demands, via heat upgrading from lower to higher temperatures. In Process Integration terms [28], this means taking heat from below the Pinch and returning it to the process above the Pinch. The current method has to assist engineers in the selection of the best HP type for a given process configuration. COP is the criterion indicating the quality of the solution because higher COP means serving the process at the expense of lower external energy input. The method follows the algorithm shown in Figure 1.

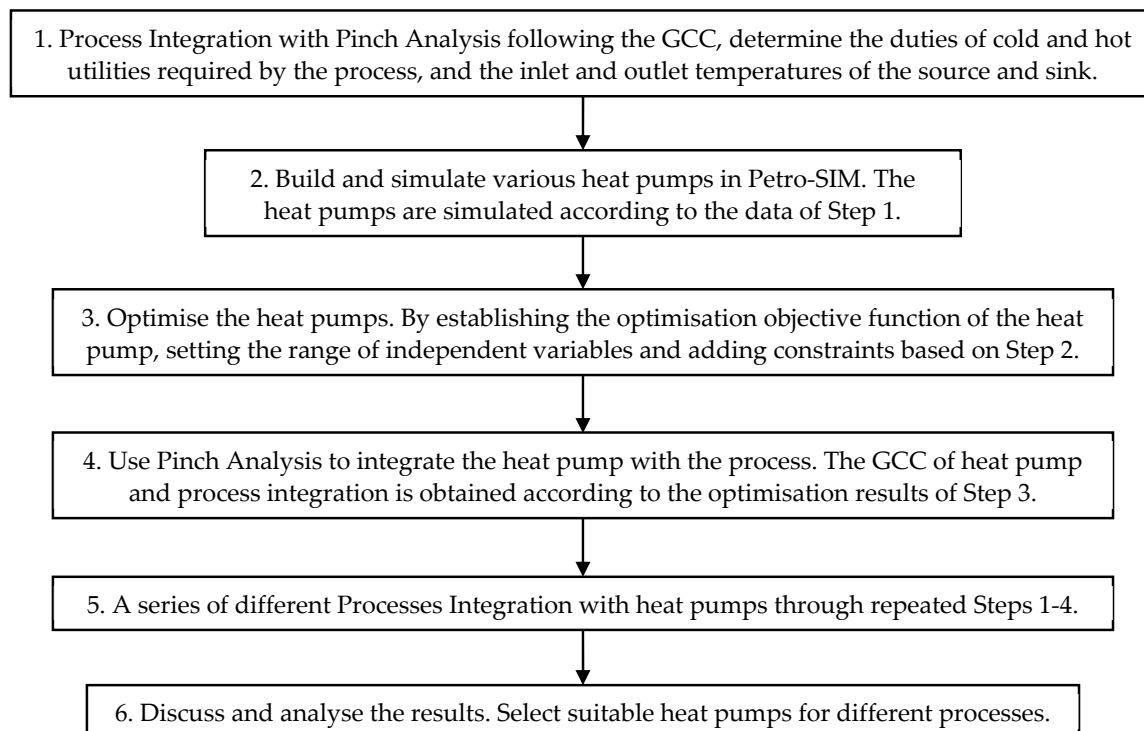


**Figure 1.** The method procedure.

### 2.1. Step 1: Process Integration with Pinch Analysis

Pinch Methodology [29] is a method to calculate thermodynamically feasible energy targets based on thermodynamic principles and analysis. The GCC [25] illustrates the difference between the heat available from hot streams and the heat required by cold streams at every temperature level, identifying

the residual heating and cooling demands of the process, to be covered by external utilities. A key property of these targets is that both loads and temperatures of the utility targets are identified. In this study, the process is firstly analysed by Pinch Analysis. The target duties of cold and hot utilities required by the process are determined, and the inlet and outlet temperatures of the heat source and heat sink for heat pumping are selected, using the GCC.

## 2.2. Step 2: Build and Simulate Different Heat Pumps

The HPs are simulated according to the data of the heat source and heat sink of Step 1. It takes the temperatures and the required heating or cooling duty of the process. In this work, JCHP, VCHP, and TCHP have been simulated by Petro-SIM [27], as shown in Figure 2. The use of Petro-SIM is similar to Aspen Hysys, as both are fork projects of the Hyprotech Hysys versions in the past. The main advantage of using Petro-SIM is that KBC has added dedicated modelling components for energy-related process units, such as boilers, turbines, compressors and HPs.

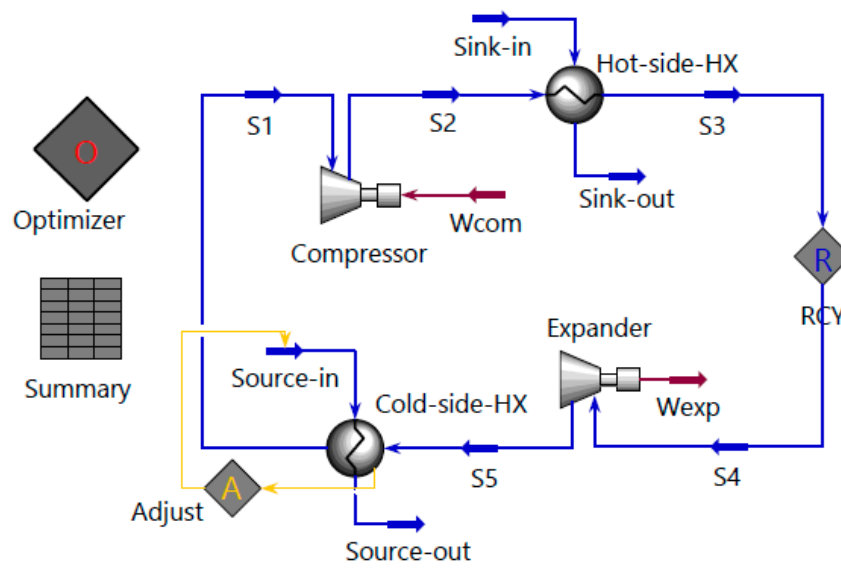
Fluid packages are based on the Peng-Robinson model [30] in combination with the Lee–Kesler Equation of State as a standard package in Petro-SIM.

Referring to the cases in Figure 2 the similarities between the three different HP cycles are as follows.

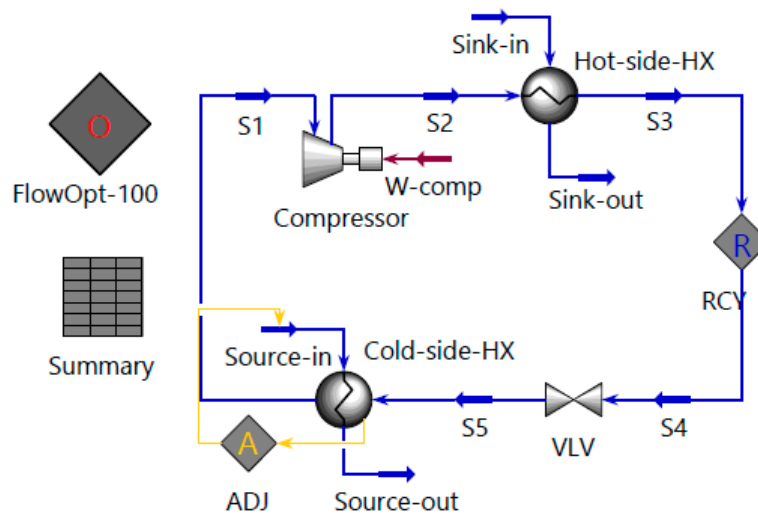
- The working fluid enters the Compressor to increase the pressure and temperature.
- The working fluid then heats the Process Heat Sink (the sink) in a heat exchanger (HX unit named “Hot-side-HX”) and is cooled down.
- Then the pressure and temperature of the working fluid are reduced through the Expander or let-down valve (VLV).
- At the next step, working fluid absorbs heat from the Process Heat Source (the source) in a Cold-side-HX or Evaporator unit.
- The working fluid finally returns to the Compressor to complete the cycle.

A critical difference is that the working fluid of a JCHP always maintains the working fluid in a gaseous state. After being cooled by the Sink, the working fluid, generates work through the Expander in the JCHP, as shown in Figure 2a, instead of using a let-down valve as in the other two cycles. In a VCHP, the working fluid has a phase change in both heat exchangers. In the Hot-side-HX, it is condensed from a gas to a liquid phase. In the Cold-side-HX, it is heated from the liquid phase to the gas phase, as shown in Figure 2b. In a TCHP, an intermediate heat exchanger is often added, and the working fluid follows a transcritical cycle, as shown in Figure 2c.

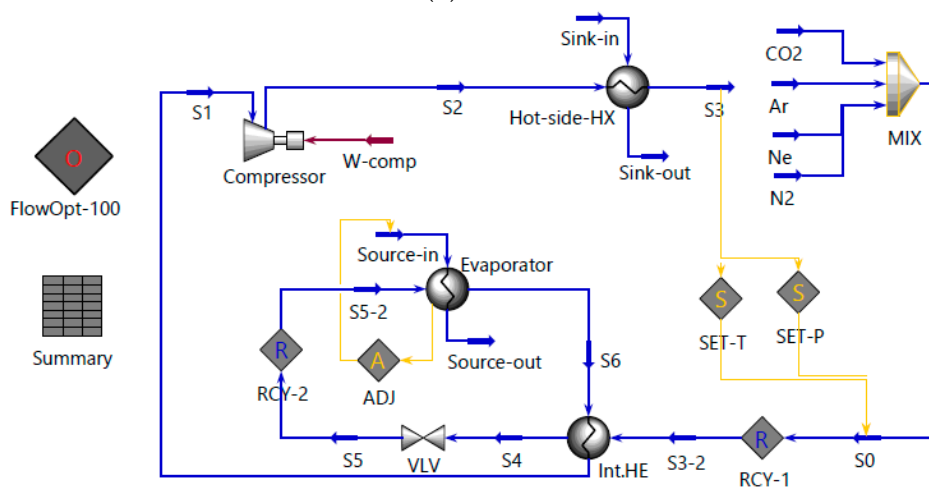
To make the simulated HP reflecting the performance of the real HP very closely, it is necessary to specify reasonable values of the device parameters in the simulation case, matching as close as possible the HP cycle and its measured indicators—mainly temperatures, pressures of the working fluid, the minimum approach temperature ( $\Delta T_{\min}$ ) of the heat exchangers and the isentropic efficiency of the compressor and expander. ECOP [23] has developed a special rotation HP with embedded compressor/expander that achieves high entropy efficiency for a JCHP. In this study, the JCHP model adopts the performance characteristics of that specific compressor/expander [23]. A common turbocompressor unit is used as the compressor of VCHP and TCHP, which is the most used type for industrial-scale HPs [31]. A formula for the relationship between the isentropic efficiency and compression ratio of compressors was proposed by Wang et al. [32]. It is assumed that the recoverable waste heat duty of process streams is known to recover waste heat of process in this study. This can be achieved by a “Adjust” unit (ADJ; Figure 2) to regulate the flow of the working fluid or source to fix the heat duty of the Cold-side-HX when the process stream as the source for a HP. When the process stream as the sink of a HP, this can be achieved by adjusting the flow of the working fluid or sink to fix the heat duty of the Hot-side-HX.



(a) JCHP



(b) VCHP



(c) TCHP

**Figure 2.** Simulation flowsheet of the heat pump as output from Petro-SIM: (a) JCHP, (b) VCHP and (c) TCHP.



### 2.3. Step 3: Optimise the Heat Pumps

Based on Step 2, the HP operating variables are optimised, and the optimal performance result is obtained by establishing the optimisation objective function of the HP, setting the range of independent variables and adding constraint conditions of the equation in Petro-SIM. It is necessary to optimise the HP based on the simulation to obtain its best performance. Petro-SIM has a multivariable optimiser. The optimiser can be used to optimise selected independent variables within defined ranges when a simulation converges, to minimise or maximise the objective function. The optimisation functionality of Petro-SIM can manipulate multiple process variables. It can be used for constrained optimisation expression with some flexibility, such as solving the objective function to maximise profit or minimise utility consumption. The iterative calculation method of the Optimiser in Petro-SIM is based on the IPOPT solver [27]. In this study, the HP system is optimised by adding an Optimiser unit in the Petro-SIM simulation. In the Optimiser, the independent variables, objective and constraints are defined to perform the optimisation. In this study, the optimisation independent variables were set as the outlet pressure (or temperature) of the Compressor and the outlet pressure (or temperature) of the Expander/VLV. The constraints are set as the  $\Delta T_{\min}$  of the HXs. The optimisation objective function is COP of the HP. The performance of a HP is generally evaluated by the COP. The COP of a HP is defined in Equation (1) [33].

$$COP = \frac{Q_h}{W} \quad (1)$$

and

$$W = Q_h - Q_c \quad (2)$$

where:  $Q_h$ —Heat output of the heat pump, kW;  $W$ —Electrical or power consumption of the HP, kW.

The identification of the HP behaviour and best performance is performed by maximising the COP value of the HP under consideration, using the model set up in Petro-SIM [27]. The specifications of the temperatures and duties are varied within ranges expected from the considered process type, and the behaviour of the system is investigated. The procedure then provides the best HP—process configuration with the optimal values of the pressures after the compressor and the expander of the selected HP.

### 2.4. Step 4: Integrate the Heat Pump with the Process

At the next step, Pinch Analysis is used to integrate the HP with the process. The placement of the HP is configured following the outcomes from the previous step. When a HP is integrated with a process, the choice of a HP system depends on the operating temperature and the heat loads below and above the Pinch. In this part, the calculation results of the HPs are plotted against the GCC of the considered process, and the optimal results are linked to the GCC profiles, including the required duties and temperatures. In this way, engineers applying the method can get a better understanding of the optimal results.

The GCC of a HP and an illustrative process is shown in Figure 3. The appropriate placement of a HP means that the heat must be recovered from below the Pinch and released above the Pinch [34]. Improper placement on either side of the Pinch will result in lower energy efficiency. The figure has two lines representing each heat exchange between the HP and the process. The thick dashed lines represent the heat transfer taking place inside the HP block—absorbing and releasing heat. The thin dashed lines represent the heat exchange directly with the process. These form extra heat circuits for minimising the probability of contamination of the internal HP fluids. All other GCC figures in this paper follow the same convention.

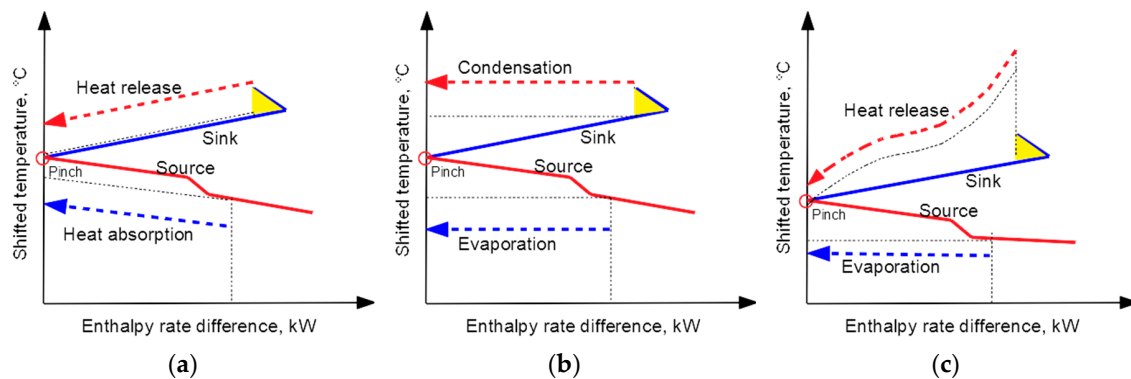


**Figure 3.** Grand Composite Curve (GCC) construction of a process with an integrated heat pump: (a) JCHP, (b) VCHP and (c) TCHP.

The example GCC of the JCHP is shown in Figure 3a. In the JCHP cycle, the working fluid remains in a gaseous state during the whole cycle of heat exchange with the process source and sink as well as the compression and expansion. This results in certain variations of the JCHP working fluid temperature. The heat absorption curve (blue dashed line) and heat release curve (red dashed line) are both oblique straight lines, as shown in Figure 3a. The working fluid slope of a JCHP is relatively large in GCC.

The example GCC of the VCHP is presented in Figure 3b. The working fluid of a VCHP is evaporated during heat exchange with the source and is condensed during heat exchange with the sink, so the phase transition occurs. The temperature of the working fluid of VCHP almost unchanged in exchange heat with the source or sink. The evaporation curve (blue dashed line) and condensation curve (red dashed line) are horizontal straight lines (i.e., minimal temperature change).

The GCC of the TCHP is shown in Figure 3c. The working fluid of TCHP is evaporated when the heat is absorbed from the process source. The heat release to the process sink takes place at supercritical conditions of the working fluid. This is why the working fluid temperature of TCHP remains constant during heat absorption from the source but changes significantly during the heat release to the sink. The evaporation curve (blue dashed line) is a horizontal straight line, whereas the heat release curve (red dashed line) is an oblique curve, as shown in Figure 3c.

### 2.5. Step 5: Evaluation of the Heat Pump Suitability to Different Process GCC Profiles

The heat duties, inlet and outlet temperatures of the heat source and sink vary among different processes. Pinch Analysis with HP placement is used, performing Steps 1–4 for a set of GCC profiles representing processes with different thermal properties. The T–H diagrams of different processes are shown in Figure 4. The configurations shown represent pairs of process heat sinks and sources of a gradual, steep and medium slope. Combinations of these are possible, but the three configurations in Figure 4 are the basic ones, which help to understand the major trends.

Each of these types of profiles implies a different degree of compatibility with the HP types considered in this work. The compatibility can be qualitatively assessed on the temperature–entropy (T–S) diagrams combining the process heat source/sink profiles with the HP profiles. Such plots are shown in Figure 5. The solid red lines represent the heat release or condensation of the working fluid in the HP, and the solid blue lines are the heat absorption or evaporation of the working fluid. The red dashed lines represent the heat release of the source, and the blue dashed lines represent the heat absorption of the sink. The performance of these three types of HPs (JCHP/VCHP/TCHP) is calculated by varying the inlet and the outlet temperatures of the process heat source and sink, and relating the results to the possible representations of temperature lifts  $\Delta T_{in}$ ,  $\Delta T_{out}$ , or  $\Delta T_1$ ,  $\Delta T_2$  (e.g., Equations (3)–(6)).

$$\Delta T_{in} = T_{sink-in} - T_{source-in} \quad (3)$$



$$\Delta T_{out} = T_{sink-out} - T_{source-out} \tag{4}$$

$$\Delta T_1 = T_{sink-in} - T_{source-out} \tag{5}$$

$$\Delta T_2 = T_{sink-out} - T_{source-in} \tag{6}$$

where:  $\Delta T_{in}$ —The inlet temperature difference of the source and sink, °C;  $\Delta T_{out}$ —The outlet temperature difference of the source and sink, °C;  $\Delta T_1$ —The difference between the inlet temperature of the sink and the outlet temperature of the source, °C;  $\Delta T_2$ —The difference between the outlet temperature of the sink and the inlet temperature of the source, °C.

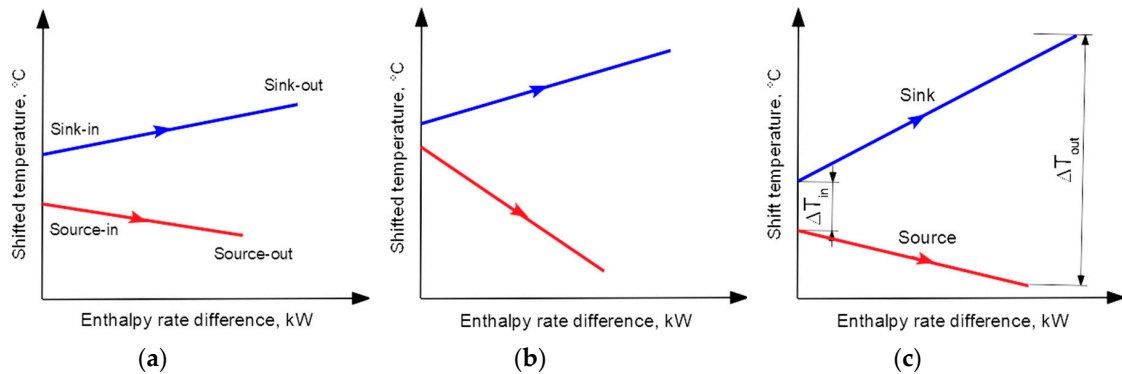


**Figure 4.** The T–H diagrams of different source and sink configurations for heat pump application. (a) Gradual slope; (b) Steep slope; (c) Medium slope.

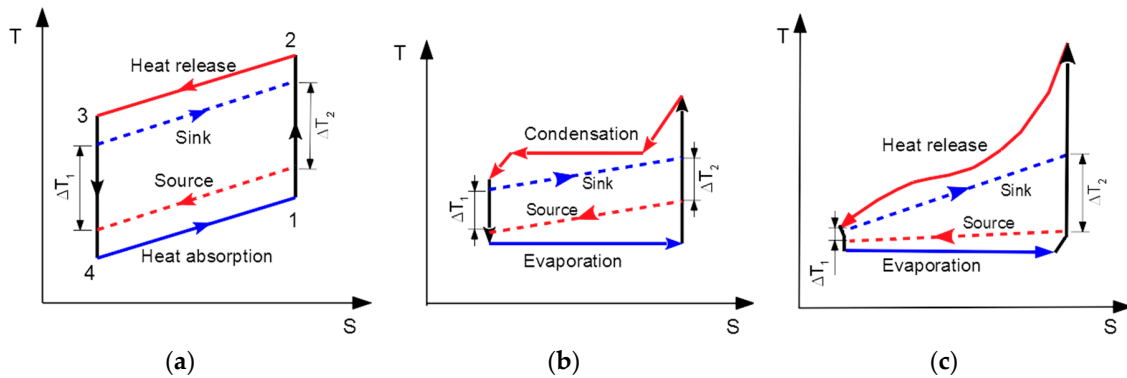


**Figure 5.** The ideal T–S diagram of the heat pumps (a) JCHP, (b) VCHP and (c) TCHP.

2.6. Step 6: Discuss and Analyse the Results

To select the HP suitable for each of the possible processes, the solutions obtained during Steps 1–5, provide engineers with sufficient information and understanding of why the proposed measures are appropriate and efficient. The evaluation is performed by the combined use of Pinch Analysis and Petro-SIM to simulate and optimise the HPs. The actions include constructing the GCC of the process and combining it with the plots of the considered HPs. The combined plots are then used for explaining the solutions and relating them to the process specifications—i.e., the temperatures and heating/cooling duties of the main process, plus the HP properties—i.e., working fluid and operating pressures.

3. Simulation and Optimisation of Heat Pumps

A series of simulations and optimisations were performed by changing the inlet and outlet temperatures of the source and sink to study the performance of these different HP cycles in different scenarios. The settings of parameters and variables of the HP are shown in Table 1.  $\Delta T_{min}$  denotes the specifications of the minimum allowed temperature differences of the heat exchangers. The pressure

differences ( $\Delta P$ ) between the stream inlets and outlets of the heat exchangers in the HP are all 50 kPa. In the “Adjust” unit, the heat transfer duty of the heat exchanger Cold-side-HX is set to 10 MW by adjusting the flowrate of stream Source-in, which is the optimisation variable. The optimisation objective is to maximise the COP. Based on the simulation results, the application range of these three types of HPs is classified and can be predicted, mapping their suitability for the various process heat source and sink scenarios.

**Table 1.** Settings of parameters and variables.

Settings		JCHP-Ar	JCHP-CO <sub>2</sub>	VCHP	TCHP
Working Fluid		Argon (Ar)	CO <sub>2</sub>	NH <sub>3</sub>	CO <sub>2</sub>
Compressor/Expander efficiency		96%	96%	65%	65%
Variable Range	<sup>1</sup> P <sub>2</sub> , MPa	3–8	2.5–7	1–7.5	7.5–20
	<sup>2</sup> P <sub>5</sub> , MPa	0.5–5	1–4	0.2–1	2–5
constraints	$\Delta T_{\min}$ of Hot-side-HX	5–30	5–30	5–30	5–30
	$\Delta T_{\min}$ of Cold-side-HX	5–30	5–30	5–30	5–30

<sup>1</sup> P<sub>2</sub>—The outlet pressure of the compressor in the HP cycle, MPa. <sup>2</sup> P<sub>5</sub>—The outlet pressure of the expander or expansion valve in the HP cycle, MPa.

The simulation results of the considered scenarios are shown in Figures 6 and 7. In Figure 6, the performance as a function of the temperature lifts expressed as the inlet and outlet temperature differences is evaluated. Figure 7 provides an evaluation of the COP as a function of the temperature lift expressed as  $\Delta T_1$  and  $\Delta T_2$ .

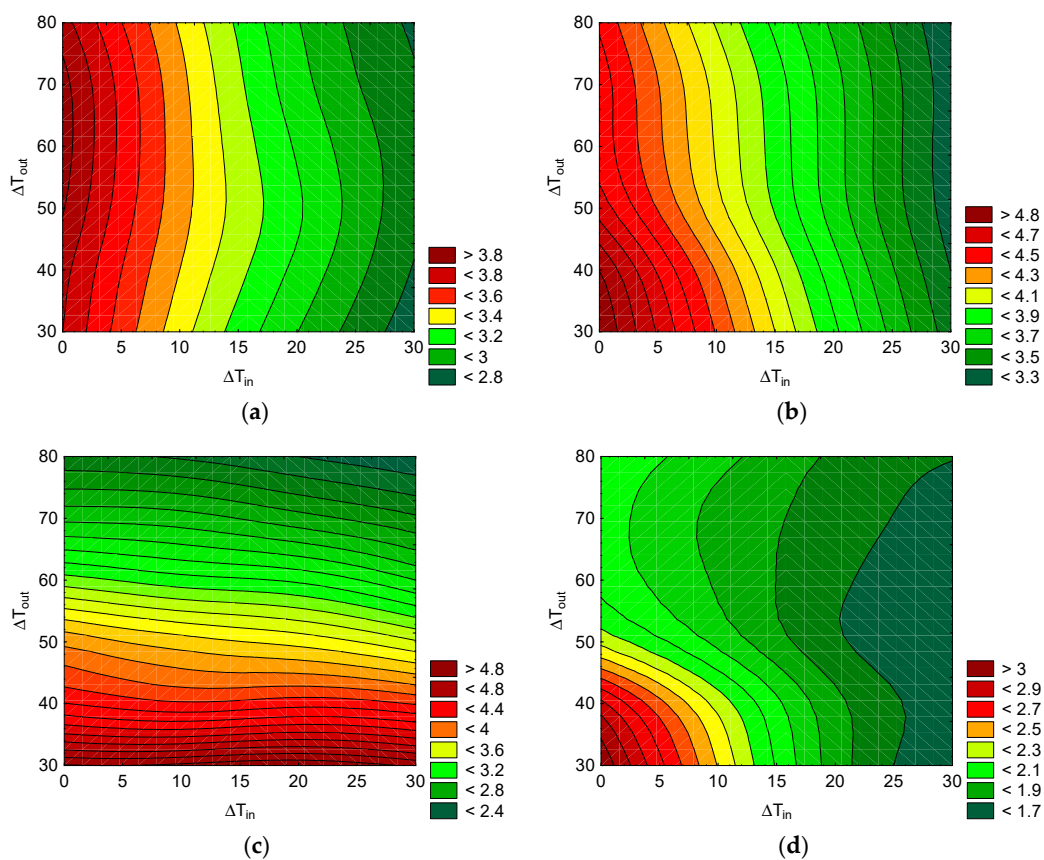


**Figure 6.** COP of different heat pumps varies with  $\Delta T_{in}$  and  $\Delta T_{out}$ : (a) JCHP-Ar, (b) JCHP-CO<sub>2</sub>, (c) VCHP and (d) TCHP.

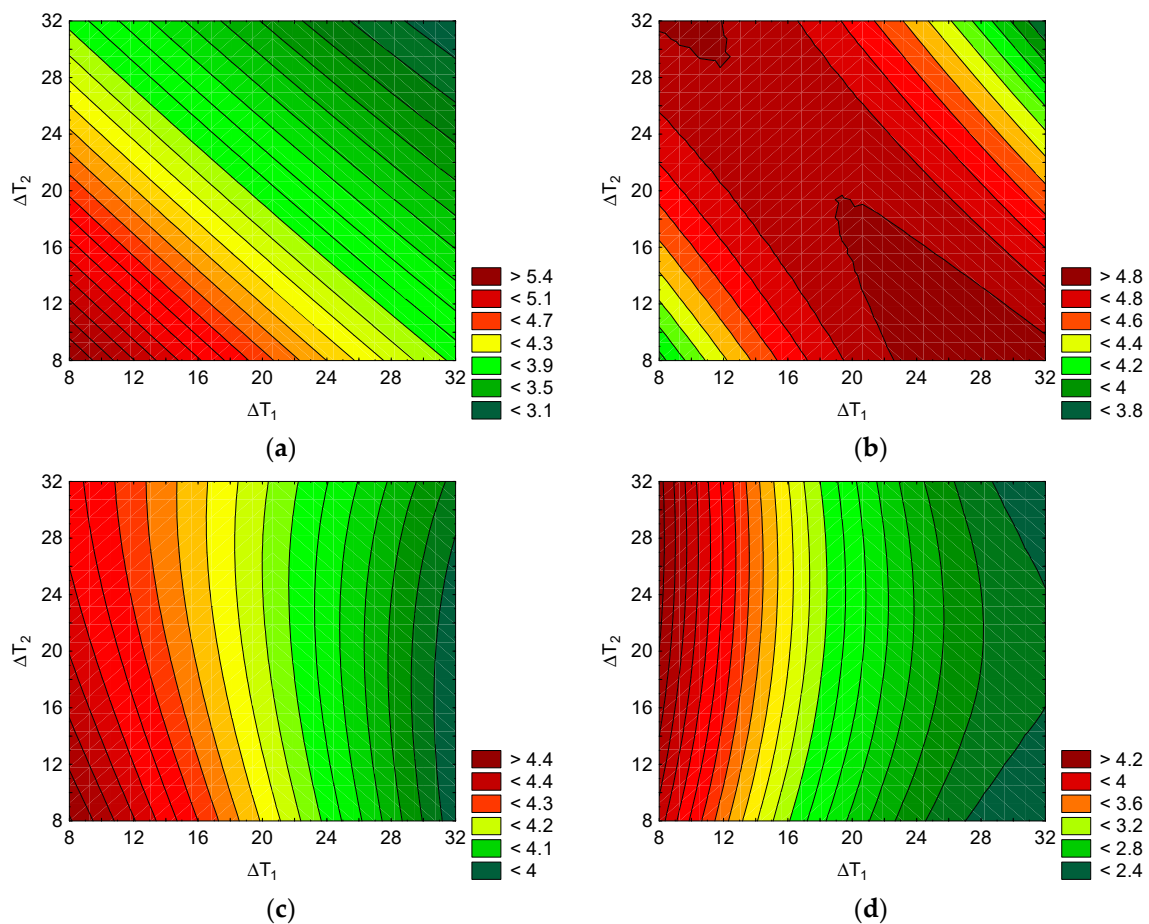


**Figure 7.** COP of different heat pumps varies with  $\Delta T_1$  and  $\Delta T_2$ : (a) JCHP-Ar, (b) JCHP-CO<sub>2</sub>, (c) VCHP and (d) TCHP.

Case 1. COP modelled as a function of the temperature lift represented by  $\Delta T_{in}$  and  $\Delta T_{out}$

The variation of COP of different HPs with  $\Delta T_{in}$  and  $\Delta T_{out}$  is shown in Figure 6. As can be seen from Figure 6a, when  $0\text{ }^{\circ}\text{C} < \Delta T_{in} < 30\text{ }^{\circ}\text{C}$  and  $30\text{ }^{\circ}\text{C} < \Delta T_{out} < 80\text{ }^{\circ}\text{C}$ , the COP of JCHP-Ar decreased with the increase of  $\Delta T_{in}$ , but did not change much with  $\Delta T_{out}$ . The COP of JCHP-CO<sub>2</sub> decreased with the increase of  $\Delta T_{in}$  but did not change much with  $\Delta T_{out}$ , as Figure 6b illustrates. This indicates that, when the inlet temperature difference ( $\Delta T_{in}$ ) between the heat source and sink is not significant, even if the outlet temperature difference ( $\Delta T_{out}$ ) between the two is very large (such as  $\Delta T_{out}$  increasing to  $80\text{ }^{\circ}\text{C}$ ), the COP of the actual JCHP is still very high. It can be seen that the JCHP is very suitable for processes where the  $\Delta T_{out}$  is massive, and  $\Delta T_{in}$  is small. The smaller  $\Delta T_{in}$ , the higher is the COP of JCHP.

When  $0\text{ }^{\circ}\text{C} < \Delta T_{in} < 30\text{ }^{\circ}\text{C}$  and  $30\text{ }^{\circ}\text{C} < \Delta T_{out} < 80\text{ }^{\circ}\text{C}$ , the COP of the evaluated VCHP decreased with the increase of  $\Delta T_{out}$ , but did not change much with  $\Delta T_{in}$ , as can be detected from Figure 6c. Therefore, when  $\Delta T_{out}$  between the source and sink is small, even if the  $\Delta T_{in}$  between the two is significant (the maximum  $\Delta T_{in}$  can only be equal to the  $\Delta T_{out}$ ), the COP of the actual VCHP is higher. The observations imply that VCHP is very suitable for processes where the temperature difference ( $\Delta T$ ) between the heat source and sink is not large. The smaller  $\Delta T_{out}$ , the higher is the COP of VCHP.

The COP of the evaluated TCHP decreased with the increase of  $\Delta T_{out}$  and  $\Delta T_{in}$  when  $0\text{ }^{\circ}\text{C} < \Delta T_{in} < 30\text{ }^{\circ}\text{C}$  and  $30\text{ }^{\circ}\text{C} < \Delta T_{out} < 80\text{ }^{\circ}\text{C}$ , as can be detected from Figure 6d. The observations imply that the application scope of TCHP is relatively narrow. TCHP is very suitable for processes where the  $\Delta T_{in}$  is small and  $\Delta T_{out} < 40\text{ }^{\circ}\text{C}$ .

The variation trend of TCHP is not very regular, and the performance contours are less noticeable. This is because TCHP is a transcritical cycle, and the thermophysical properties of CO<sub>2</sub> in the supercritical state are nonlinear, as the substance does not behave like a gas or a liquid. This makes it necessary to model the HP behaviour also as a function of the other two temperature lift representations:  $\Delta T_1$  and  $\Delta T_2$ , by analogy with heat exchanger temperature differences and the T–S diagrams of the HP cycles.

Case 2. COP modelled as a function of the temperature lift represented as  $\Delta T_1$  and  $\Delta T_2$

The change of COP of different HPs with  $\Delta T_{in}$  and  $\Delta T_{out}$  is studied by fixing the outlet temperature of sink  $T_{sink-out}$  to a certain level. In this study the  $T_{sink-out}$  is set as 50 °C. When  $T_{sink-out}$  is 50 °C, the change of COP of the different HPs with  $\Delta T_1$  and  $\Delta T_2$  is shown in Figure 7. It can be seen that the COP of JCHP-Ar decreased with the increase of  $\Delta T_1$  and  $\Delta T_2$ . The COP of JCHP-CO<sub>2</sub> first increased and then decreased with the increase of  $\Delta T_1$  and  $\Delta T_2$ , featuring a maximum. The COP of VCHP and TCHP decreased with the increase of  $\Delta T_1$ , but did not change much with  $\Delta T_2$ .

It can be seen from Figure 7d that when the temperature difference  $\Delta T_1$  is small, even if the temperature difference  $\Delta T_2$  is large, the COP of the TCHP is higher. The TCHP is then very suitable for a small temperature rise  $\Delta T_1$  (preferably  $\Delta T_1 \leq 10$  °C) combined with a large  $\Delta T_2$  process.

In conclusion, the observations imply from Figures 6 and 7 that JCHP is very suitable for the process of steep T–H lines of the source and sink in GCC. VCHP suitable for selection when the slopes of the T–H lines of the source and sink have a relatively low gradient (closer to flat). TCHP suitable for selection when the slope of the T–H line of the source have a relatively low gradient (closer to flat) and steep T–H line of the sink in GCC.

#### 4. Case Studies

This section analyses the integration of the different types of HPs using industrial examples to assess the practicability of the conclusion of Section 3. The optimisation objective function is the COP of the HP.

##### 4.1. Formulation and Development: Process Integration Using JCHP, VCHP and TCHP

Four different industrial processes have been studied. The first process is a spray drying process of milk powder in a dairy factory [35], and its GCC is shown in Figure 8. The second process is also from dairy product processing [36], which uses raw milk to produce concentrated milk, pasteurised milk, cream, yoghurt and dessert. The GCC for that is shown in Figure 9. The third example is from candy processing and packaging in a candy factory [37]. The GCC is shown in Figure 10. The fourth process is a 4-column double-effect methanol distillation in a chemical plant [38]. The GCC is shown in Figure 11. The  $\Delta T_{min}$  between the heat source/sink and the working fluid in the HP cycle is 5 °C. The compressors and expanders of the JCHP adopt centrifugal force rotating system structure, and their isentropic efficiency can be as high as 96%. The compressors of VCHP and TCHP are ordinary turbocompressors. In this study, isentropic efficiency is assumed to be 65%.

##### 4.1.1. Case 1: Milk Spray Drying Process

The spray drying process of the milk powder was integrated with the HP. The stream data were only adopted the spray drying process from Atkins et al. [35], as shown in Table 2. The  $\Delta T_{min}$  of the process is 20 °C.

**Table 2.** The stream data from a spray drying process.

Steam Name	Type	$T_s, ^\circ\text{C}$	$T_t, ^\circ\text{C}$	CP, kW/ $^\circ\text{C}$
Milk Concentrate	Cold	54	65	37.6
Dryer Inlet Air	Cold	25	200	119.2
Fluid Bed A Inlet Air	Cold	25	50	10.2
Fluid Bed B Inlet Air	Cold	25	45	14.9
Fluid Bed C Inlet Air	Cold	25	32	11.2
Air Exhaust	Hot	75	20	174.7

As can be seen from the GCC in Figure 8, the Pinch Temperature of this process is  $65\text{ }^\circ\text{C}$ . The hot utility required is 17.66 MW and the cold utility required is 5.36 MW. It is assumed that all the source energy is used to heat the sink when the process is integrated with a HP. The heat duty of the heat exchanger at the source side for the HP is fixed 5.36 MW. The allowed range of the independent variables and the optimisation results of a spray dryer with an integrated HP (maximising the COP) are shown in Table 3.

**Table 3.** Variation settings and optimisation results of a spray drying with an integrated heat pump.

Heat Pump	Variation Ranges			Optimisation Results				
	$^1 P_2, \text{MPa}$	$^2 P_5, \text{MPa}$	COP, -	$Q_{\text{sink}}, \text{MW}$	W, MW	$P_2, \text{MPa}$	$P_5, \text{MPa}$	$^3 R, -$
JCHP-Ar	5–9	2–5	2.83	8.29	2.93	8.99	4.35	2.09
JCHP-CO <sub>2</sub>	4–7	1–3	2.93	8.04	2.74	6.47	1.70	3.92
VCHP	2.5–9	0.2–1	1.85	11.66	6.30	8.01	0.51	17.40
TCHP	12–20	2–5	1.77	12.11	6.83	18.65	3.03	6.27

<sup>1</sup>  $P_2$ : The outlet pressure of the compressor in the HP cycle, MPa. <sup>2</sup>  $P_5$ : The outlet pressure of the expander or expansion valve in the HP cycle, MPa. <sup>3</sup> R: The compression ratio of the compressor, -.

For evaluation and interpretation, the GCC of the process integrated with different types of HPs is given, as shown in Figure 8. As can be seen from Table 3, the four HPs (JCHP-Ar, JCHP-CO<sub>2</sub>, VCHP and TCHP) can save 47%, 46%, 66% and 69% of the hot utility by improving the waste heat quality of the process. The ranking of best COP of the HPs is JCHP-CO<sub>2</sub> > JCHP-Ar > VCHP > TCHP when integrating with this process. The reason can be seen in Figure 8, showing that the inlet temperature difference  $\Delta T_{\text{in}}$  between source and sink is too small, while the outlet temperature difference  $\Delta T_{\text{out}}$  is too large. That is, the slopes of source and sink are both steep in the GCC.

In the HP cycle, the working fluid of the JCHP does not undergo a phase change and remains in the gas phase. As a result, the  $\Delta T$  between the inlet and the outlet of the working fluid in the JCHP changes significantly in the heat exchange with source or sink. The slope of the working fluid is relatively large in GCC, as shown in Figure 8a,b.

The working fluid of VCHP is evaporated during heat exchange with the source and is condensed during heat exchange with the sink, so the phase transition occurs. Therefore, in the heat exchange with the source or sink, the  $\Delta T$  between the inlet and the outlet of the working fluid in the VCHP changes a little. The slope of the working fluid is small in GCC, as shown in Figure 8c. The reason for the temperature difference in the red dashed line in Figure 8c is that the working fluid becomes a superheated gas after increasing the pressure by the compressor. In the heat exchanger hot-side-HX, the working fluid is cooled to a saturated gas and then condensed to a liquid. Therefore, the red dashed line is tilted first and then becomes horizontal. However, when the working fluid is a gas that cools down from the superheated state to the saturated state, the CP is small, and the heat exchange efficiency is low. At the same time, the sink is a gas that the CP is small and the sink slope is large during the heat exchange, so the oblique part of the red dashed line is longer.

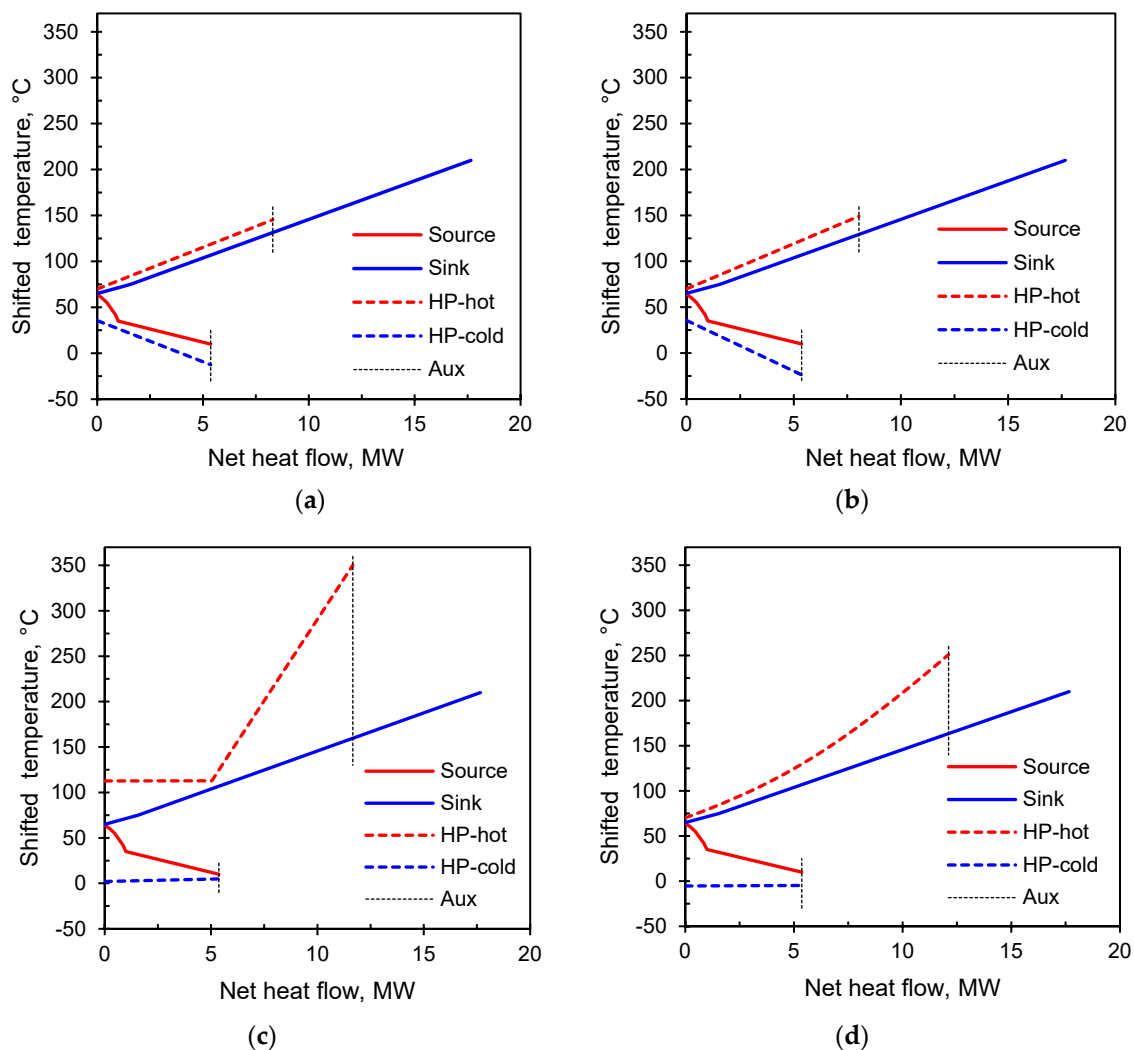


**Figure 8.** GCC of Case 1 and Process Integration using (a) JCHP-Ar, (b) JCHP-CO<sub>2</sub>, (c) VCHP and (d) TCHP.

The working fluid of TCHP is evaporated during exchanging heat with the source, while is supercritical fluid during heat transfer with the sink. As the slope of the working fluid is small during the heat transfer with the source in the GCC, whereas the slope of the working fluid is significant in the heat exchange with sink in the GCC, as shown in Figure 8d. In this case, the average temperature between working fluid and source/sink in JCHP is small, so the energy loss of the heat exchangers is lower, the heat exchange efficiency is higher, and affects the COP positively. The average temperature between the working fluid and the source/sink in VCHP and TCHP is large, so the energy loss is higher, the heat exchange efficiency is smaller and affects the COP negatively. The performance of VCHP and TCHP are both weak. In addition, the compression ratio of the compressor in VCHP is 17.40 too high for a single stage. This means that multiple stages of compression would be required, resulting in a substantial increase in the cost of the compressor and a higher cost for VCHP. The outlet pressure of the compressor in TCHP is very high (18.65 MPa). This means high-pressure requirements for equipment of TCHP, with very high equipment investment costs. The economy of the VCHP and TCHP are both weak, and this process is more suitable for Heat Integration with JCHP, which is consistent with the conclusion of Section 3. It can be seen that the method proposed in this study is feasible and effective.



#### 4.1.2. Case 2: Raw Milk Processing into Dairy Products

The stream data are taken from Wallerand et al. [36], as shown in the Appendix A (Table A1). The  $\Delta T_{\min}$  of the process is 4 °C. As can be seen from the GCC in Figure 9, the Pinch Temperature of this process is 66.9 °C. The hot utility required is 2.34 MW and the cold utility required is 0.94 MW. It is assumed that the heat duty of the heat exchanger at the source side is fixed 0.71 MW. Both the process heat source and the sink undergo a phase transition. The source needs to be condensed, and the sink needs to be heated and evaporated. The pressure differences of the heat exchangers on the source side and sink sides are both set 0 kPa. The setting range of independent variables and optimisation results of HP integration into a dairy product process are shown in Table 4.

**Table 4.** Variable settings and optimisation results of a dairy product with an integrated heat pump.

Heat Pump	Variable Ranges			Optimisation Results				
	<sup>1</sup> P <sub>2</sub> , MPa	<sup>2</sup> P <sub>5</sub> , MPa	COP, -	Q <sub>sink</sub> , MW	W, MW	P <sub>2</sub> , MPa	P <sub>5</sub> , MPa	<sup>3</sup> R, -
JCHP-Ar	5–9	3–5	3.89	1.00	0.26	6.97	4.87	1.45
JCHP-CO <sub>2</sub>	4–8	1–4	4.52	0.92	0.20	4.37	2.56	1.74
VCHP	3.5–7	0.5–3	13.07	0.77	0.05	3.62	2.73	1.35
TCHP	14–20	2–5	1.68	1.81	1.08	17.54	3.03	5.89

<sup>1</sup> P<sub>2</sub>: The outlet pressure of the compressor in the HP cycle, MPa. <sup>2</sup> P<sub>5</sub>: The outlet pressure of the expander or expansion valve in the HP cycle, MPa. <sup>3</sup> R: The compression ratio of the compressor.

The GCC of the dairy products process integrated with different types of HPs is shown in Figure 9. As can be seen from Table 4, the four HPs (JCHP-Ar, JCHP-CO<sub>2</sub>, VCHP, and TCHP) can save 43%, 39%, 33%, and 78% of the hot utility by improving the waste heat quality of the process. The ranking of the HP COPs is VCHP > JCHP-CO<sub>2</sub> > JCHP-Ar > TCHP when integrating with the dairy products process.

The reason can be seen in Figure 9. The  $\Delta T_{\text{in}}$  and the  $\Delta T_{\text{out}}$  between the source and the sink are both too small (1.5 °C). The slopes of both the source and sink in the GCC plot are too small (flat). As the working fluid of the JCHP remains a gas across the whole HP cycle, the  $\Delta T$  between the inlet and the outlet of the working fluid in the JCHP varies significantly in the heat exchange with source or sink. The slope of the working fluid is relatively large in the GCC, as shown in Figure 9a,b. As the working fluid of the VCHP is evaporated during heat exchange with the source and is condensed during heat exchange with the sink, the  $\Delta T$  between inlet and outlet of the working fluid in the VCHP does not change in the heat exchange with the source or sink. The slope of the working fluid is small in the GCC, as shown in Figure 9c. The working fluid of TCHP is evaporated during exchanging heat with the source, whereas it is a supercritical fluid during the heat transfer to the sink. Therefore, the slope of the working fluid is small in the heat exchange with the source in the GCC, while the slope of the working fluid is steep in the heat exchange with sink in GCC, as shown in Figure 9d. In this case, the average temperature between the working fluid and the source/sink in VCHP is small, so the energy loss of the heat exchangers is lower, the heat exchange efficiency is higher and affects COP positively. Although the average temperature between working fluid and source/sink in JCHP and TCHP is large, so the energy loss is higher, the heat exchange efficiency is smaller, and affects negatively to the COP. The performance of JCHP and TCHP are both weak. In addition, the outlet pressure of the compressor in TCHP is too high (17.54 MPa). This means high-pressure requirements for equipment of TCHP, with very high equipment investment costs. The TCHP economy is weak. This process is more suitable for Heat Integration with VCHP, which is consistent with the conclusion of Section 3. It can be seen that the method proposed in this study is feasible and effective.

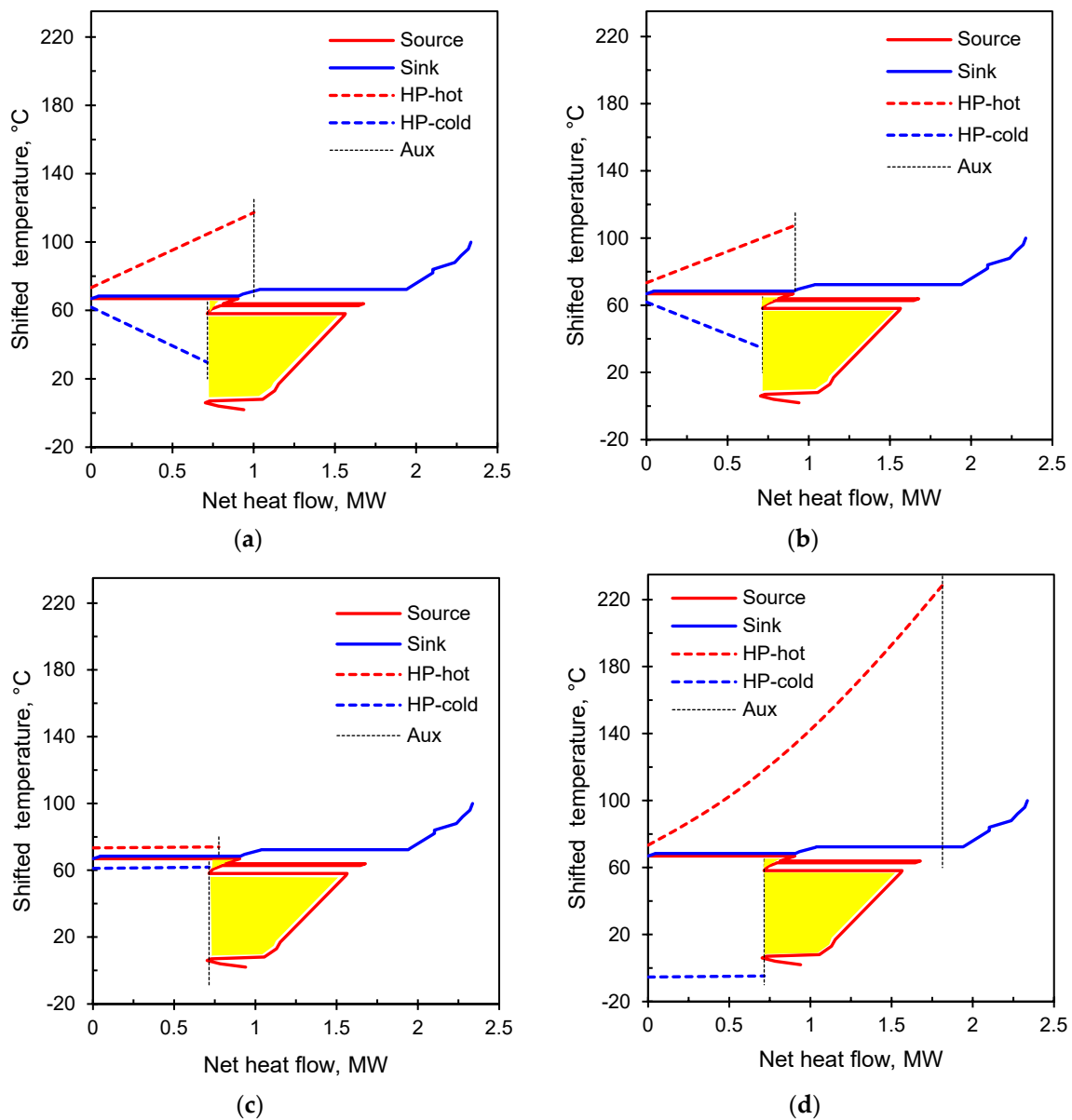


**Figure 9.** GCC of case 2 with integration options using (a) JCHP-Ar, (b) JCHP-CO<sub>2</sub>, (c) VCHP and (d) TCHP.

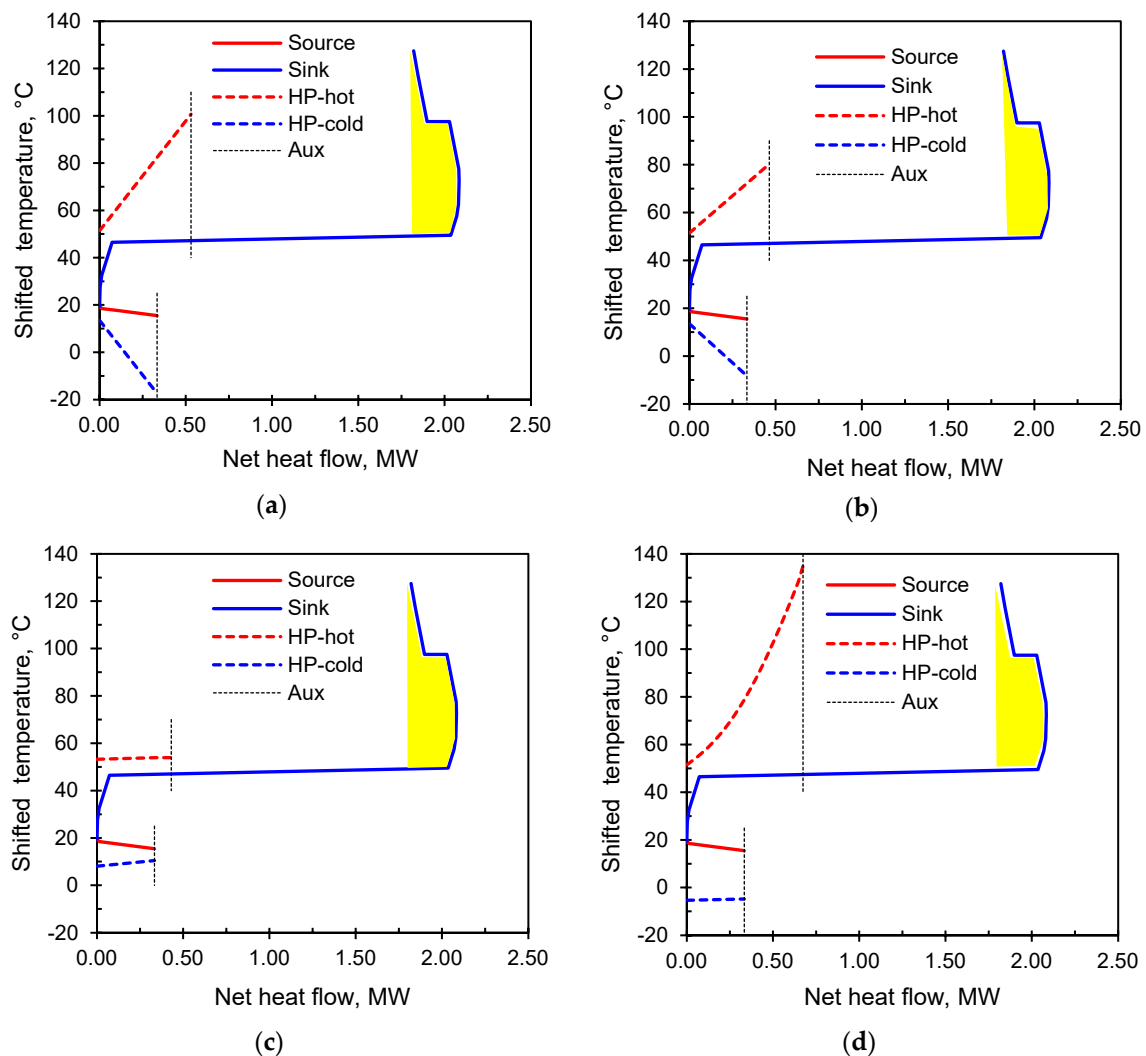
#### 4.1.3. Case 3: Candy Processing and Packaging

The process of candy processing and packaging was evaluated for HP integration. The stream data were taken from Miah et al. [37] and are listed in the Appendix A (Table A2). The  $\Delta T_{\min}$  of the process is 5 °C. As can be seen from the GCC in Figure 10, the Pinch temperature of this process is 19.5 °C. The hot utility required is 1.82 MW and the cold utility required is 0.33 MW. It is assumed that all the source energy is used to heat the sink when the process is integrated with a HP, fixing the source duty to 0.33 MW. The pressure differences of the heat exchangers on the source side and sink sides are both 50 kPa. The setting ranges of the independent optimisation variables and optimisation results of a process of candy processing and packaging integration HP are shown in Table 5.

**Table 5.** Variable settings and optimisation results of a process of candy processing and packaging integration heat pump.

Heat Pump	Variable Ranges		Optimisation Results					
	<sup>1</sup> P <sub>2</sub> , MPa	<sup>2</sup> P <sub>5</sub> , MPa	COP, -	Q <sub>sink</sub> , MW	W, MW	P <sub>2</sub> , MPa	P <sub>5</sub> , MPa	<sup>3</sup> R, -
JCHP-Ar	5–9	3–5	2.81	0.53	0.19	7.05	3.75	1.90
JCHP-CO <sub>2</sub>	4–7	1–4	3.55	0.46	0.13	6.13	2.65	2.36
VCHP	1.5–7	0.5–2	4.44	0.43	0.10	2.25	0.62	3.95
TCHP	9–15	2–5	1.85	0.67	0.36	10.75	3.03	3.61

<sup>1</sup> P<sub>2</sub>: The outlet pressure of the compressor in the HP cycle, MPa. <sup>2</sup> P<sub>5</sub>: The outlet pressure of the expander or expansion valve in the HP cycle, MPa. <sup>3</sup> R: The compression ratio of the compressor, -.

**Figure 10.** GCC of case 3 and integration options using (a) JCHP-Ar, (b) JCHP-CO<sub>2</sub>, (c) VCHP and (d) TCHP.

For intuitive display of the results and analysis, the GCC of the process combined with the HPs is shown in Figure 10. As can be seen from Table 5, the four HPs (JCHP-Ar, JCHP-CO<sub>2</sub>, VCHP and TCHP) can save 29%, 25%, 24% and 37% of the hot utility by improving the waste heat quality of the process. The ranking of the HP COPs is VCHP > JCHP-CO<sub>2</sub> > JCHP-Ar > TCHP when integrating with this process. The reason can be seen in Figure 10, stemming from the fact that the  $\Delta T_{in}$  between the source and the sink is approximately the same as the  $\Delta T_{out}$ . The slopes of source and sink are

both small in the GCC. As the working fluid of the JCHP does not undergo a phase change remaining gas, the  $\Delta T$  between inlet and outlet of the working fluid in JCHP changes significantly in the heat exchange with both the source and the sink. The slope of the working fluid is relatively large in the GCC (Figure 10a,b). Due to the phase changes of the working fluid of the VCHP, the  $\Delta T$  between the inlet and outlet of the working fluid in the VCHP change very little. The slope of the working fluid is small in the GCC, see Figure 10c. For the TCHP, the slope of the working fluid is small in the heat exchange with source in the GCC, whereas the slope of the working fluid is large in the heat exchange with sink in the GCC, see Figure 10d.

In this case, the average temperature between working fluid and source/sink in VCHP is small, so the energy loss of the heat exchangers is lower, the heat exchange efficiency is higher and affects the COP positively. Although the average temperature between working fluid and source/sink in JCHP and TCHP is large, and therefore the energy loss is higher, the heat exchange efficiency is smaller and affects negatively the COP. The performance of JCHP and TCHP are both weak. This process is more suitable for heat integration with a VCHP, which is consistent with the conclusion of Section 3.

#### 4.1.4. Case 4: Methanol Distillation Process

The methanol distillation process was evaluated for HP integration based on the stream data from a 4-column double-effect methanol distillation process of a chemical plant [38]. The data are given in the Appendix A (Table A3). The  $\Delta T_{\min}$  of the process is 15 °C. As can be seen from the GCC in Figure 11, the Pinch Temperature of this process is 74.26 °C. The hot utility required is 138.48 MW and the cold utility required is 139.90 MW. It is assumed that the heat duty of the heat exchanger at the sink side is fixed 20.86 MW. The pressure differences of the heat exchangers at source side are set 50 kPa, and at the sink, the side is set 0 kPa. The setting range of independent variables and optimisation results of a 4-column double-effect methanol distillation with an integrated HP are shown in Table 6. Finally, for more intuitive display the results, the GCC of a 4-column double-effect methanol distillation process integrated with different types of HPs is given, as shown in Figure 11. As can be seen from Table 6, the HPs can save 15% of the hot utility by improving the waste heat quality of the process. The ranking of the HP COPs is VCHP > JCHP-CO<sub>2</sub> > JCHP-Ar > TCHP when integrating with this process. The reason can be seen in Figure 11 and is related to the observation that the  $\Delta T_{in}$  between source and sink is small, while the  $\Delta T_{out}$  is too significant. The slopes of source and sink are both steep in the GCC.

**Table 6.** Variable settings and optimisation results of a methanol distillation with an integrated heat pump.

	Variable Ranges			Optimisation Results					
	<sup>1</sup> P <sub>2</sub> , MPa	<sup>2</sup> P <sub>5</sub> , MPa	<sup>3</sup> T <sub>5</sub> , °C	COP, -	Q <sub>source</sub> , MW	W, MW	P <sub>2</sub> , MPa	P <sub>5</sub> , MPa	<sup>4</sup> R, -
JCHP-Ar	4–8	1–5	–	3.23	14.40	6.46	5.49	3.50	1.59
JCHP-CO <sub>2</sub>	4–9	1–4	–	4.02	15.03	5.19	4.92	2.55	1.97
VCHP	2.5–8	0.2–3	–	5.67	17.18	3.64	5.28	2.40	2.24
TCHP	20–30	–	–10–25	1.50	7.09	13.92	25.71	6.07	4.27

<sup>1</sup> P<sub>2</sub>: The outlet pressure of the compressor in the HP cycle, MPa. <sup>2</sup> P<sub>5</sub>: The outlet pressure of the expander or expansion valve in the HP cycle, MPa. <sup>3</sup> T<sub>5</sub>: The outlet temperature of the expansion valve in the HP cycle, MPa.

<sup>4</sup> R: The compression ratio of the compressor.

The  $\Delta T$  between the inlet and outlet of the working fluid in JCHP changes significantly in the heat exchange with both the source and the sink. The slope of the working fluid is relatively large in the GCC, as shown in Figure 11a,b. For the VCHP, in the heat exchange with the source and the sink, the  $\Delta T$  between the inlet and outlet of the working fluid in VCHP change very little. The slope of the working fluid is small in the GCC—see Figure 11c. The TCHP shows a different behaviour due to the transcritical nature of the heat release part. The slope of the working fluid is small in the heat exchange

with source in the GCC, while the slope of the working fluid is steep in the heat exchange with sink in the GCC, as shown in Figure 11d.

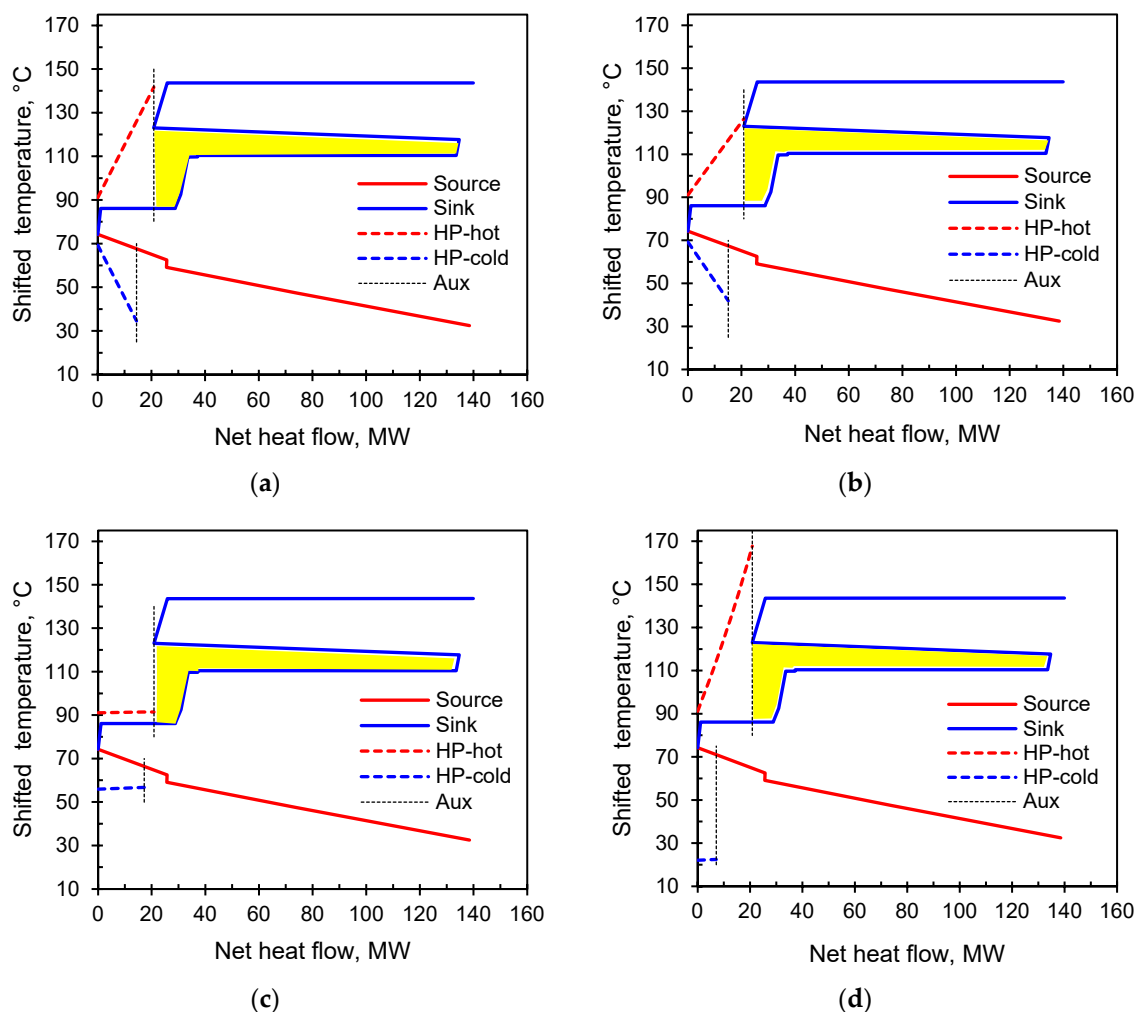


**Figure 11.** GCC of case 4 and integration options using (a) JCHP-Ar, (b) JCHP-CO<sub>2</sub>, (c) VCHP and (d) TCHP.

In this case, the average  $\Delta T$  between working fluid and source/sink in VCHP is small, so the energy loss of the heat exchangers is lower, the heat exchange efficiency is higher, and COP is affected positively. Although the average  $\Delta T$  between working fluid and source/sink in JCHP and TCHP is massive, and thus the energy loss is higher, the heat exchange efficiency is smaller, and this affects the COP negatively. The performance of the JCHP and the TCHP are both weak. In addition, the outlet pressure of the compressor in TCHP is too high (25.71 MPa). This means high-pressure requirements for equipment of TCHP, with high equipment investment cost. The TCHP economy is likely to be poor. This process is more suitable for heat integration with VCHP, which is consistent with the conclusion of Section 3.

For the optimal COP of JCHP, the reason for the large  $\Delta T$  between the working fluid and the source/sink after heat exchange can be seen in Figure 12. The figure shows the relationship between power consumption and COP of JCHP with compression ratio. In the JCHP, the heat load of the sink-side heat exchanger  $Q_h$  and the outlet pressure of the expander are fixed. By changing the outlet pressure of the compressor, a series of work required by the compressor, work produced by the expander and COP are obtained. It can be seen from Equation (1) that the COP is inversely proportional to the power consumption of the HP when  $Q_h$  is constant.

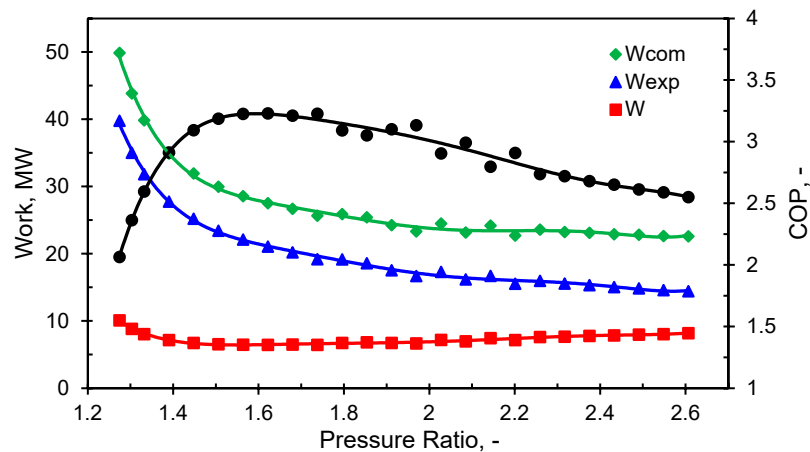


**Figure 12.** The relationship between power consumption and COP of JCHP with compression ratio.

As can be seen from Figure 12, with the increase of the compression ratio of the compressor (that is, the increase of the outlet pressure of the compressor compared to inlet pressure), the power consumption of the JCHP first decreases and then increases. The COP of JCHP increases first and then decreases with the increase of compressor compression ratio. That is, there is an optimal pressure for the optimal COP of the JCHP. When the outlet pressure of the compressor is lower than the optimal pressure, although the outlet temperature of the compressor decreases (that is, the inlet temperature of the working fluid exchanging heat with the source decreases and the temperature difference decreases), the COP of JCHP is not optimal. The same is true for the sink side.

#### 4.2. Evaluation

The results of the Heat Integration of the four industrial processes with HPs are compared. They are summarised in Table 7.

**Table 7.** The results of different industrial Processes Integration with heat pumps.

Name	Unit	Case 1: Milk Spray Drying Process	Case 2: Dairy Product Process	Case 3: Candy Processing and Packaging	Case 4: Methanol Distillation	
GCC	$T_{\min}$	°C	10	2	15.5	32.5
	$T_{\text{Pinch}}$	°C	65	66.9	19.5	74.26
	$T_{\max}$	°C	210	100	127.5	143.68
	Utility-cold	MW	5.36	0.94	0.33	138.48
	Utility-hot	MW	17.66	2.34	1.82	139.90
Source	$T_{\text{source-in}}$	°C	40.7	66.9	19.5	74.26
	$T_{\text{source-out}}$	°C	10	66.9	15.5	67
Sink	$T_{\text{sink-in}}$	°C	65	68.4	46.5	86.1
	$T_{\text{sink-out}}$	°C	–	68.4	49.5	86.1
Duty	$Q_{\text{source}}$	MW	5.36	0.71	0.33	–
	$Q_{\text{sink}}$	MW	–	–	–	20.86
COP	JCHP-Ar	–	2.83	3.89	2.81	3.23
	JCHP-CO <sub>2</sub>	–	2.93	4.52	3.55	4.02
	VCHP	–	1.85	13.07	4.44	5.67
	TCHP	–	1.77	1.68	1.85	1.50

For the processes with steep source and sink slopes, such as the spray drying process of the milk powder in a dairy factory in Case Study 1, the average  $\Delta T$  of working fluid and source/sink in JCHP is small, resulting in a small energy loss and high heat exchange efficiency. The COP of JCHP is large, so it is appropriate to choose the JCHP.



When the source and sink slope of process is gentle or (nearly) flat, for example, as in the dairy product processing of Case Study 2 and the candy processing and packaging in Case Study 3, the VCHP is most suitable because the average  $\Delta T$  of the working fluid and source/sink are small, the energy loss is small resulting in high thermal efficiency and high COP values. In Case Study 2, the  $\Delta T_{in}$  is as low as 1.5 °C, and the COP of VCHP is as high as 13.07.

From Case Study 2 to Case Study 3, the  $\Delta T_{in}$  increased from 1.5 °C to 11.84 °C, and the COP of the VCHP decreased from 13.07 to 4.44. Therefore, the smaller the  $\Delta T_{in}$  between source and sink is, the larger is the COP of the VCHP. The COP of the VCHP decreased rapidly with the increase of  $\Delta T_{in}$  between source and sink. However, the COP of JCHP decreased less with the increase of  $\Delta T_{in}$  between source and sink.

The application scope of the TCHP is limited. The TCHP is more appropriate for a process with a relatively gentle source slope and a relatively steep sink slope. The best process is one which the inlet temperature of the source is less than or equal to 20 °C, and the  $\Delta T_{in}$  between the source and sink is less than 10 °C.

## 5. Conclusions

Several main types of HPs have been critically analysed for obtaining rules and criteria on appropriate HP selection for various process configurations. In addition to the relatively recent JCHP, other HP types are in use and have been industrialised, including the VCHP and TCHP types. This paper performs a comparative evaluation of the performance of the Heat Integration scenarios of different HP types (VCHP, TCHP and JCHP) and processes, by applying the Petro-SIM process simulator and Pinch Analysis.

An answer is provided to the question of which type of HP is most suitable for a specific process. The results show that for processes with larger source and sink slopes on the T–H plot, the COP of JCHP is higher, and JCHP is more suitable. For processes with a relatively smaller and medium slope of the source and sink T–H profiles, the COP of VCHP is relatively large, and VCHP is more suitable. The scope of application of TCHP is small.

For processes with a relatively low source T–H slope and a relatively large sink T–H slope, the COP of TCHP is more substantial, and it is appropriate to select it. Because the critical temperature of CO<sub>2</sub> is 31.26 °C, the added constraint in this context is a process for which the source inlet temperature is lower than 20 °C, the sink temperature requires more than 40 °C, and the  $\Delta T_{in}$  between the source and the sink is less than 10 °C.

By improving the waste heat quality of the process, the HPs can save 15 to 78% of the hot utility. The smaller the  $\Delta T_{in}$  between source and sink is, the larger is the COP of the VCHP. The  $\Delta T_{in}$  increased from 1.5 °C to 11.84 °C, and the COP of the VCHP decreased from 13.07 to 4.44. The COP of the VCHP decreased rapidly with the increase of  $\Delta T_{in}$  between source and sink. However, the COP of JCHP decreased less with the increase of  $\Delta T_{in}$  between source and sink.

It is shown that if an inappropriate HP is selected to integrate with the process, the COP of the HP would decline, which may lead to an increase in investment and a decrease in the economy of the HP. In the extreme cases, the differences between the most and the least suitable integration mappings can be of the order of 100% and up to tenfold. This shows the importance of performing such an analysis and making the correct choice of a HP.

For the different scenarios of Heat Integration with HPs, this study can provide guidance and suggestions for the selection of HPs, enabling a quick selection of the appropriate HPs. A simplifying assumption for the current work is the use of the COP of the HP—process combinations as the performance criterion, and considering the investment cost of HPs only qualitatively. The full analysis, relaxing this assumption and considering the investment and analysis of the economy is planned for future work. The future research will be targeted to find the balance between the COP and the economy of the HP application.

**Author Contributions:** L.G. has written the draft performing the complete study at the previously published idea of T.G.W. to extend the comparison of heat pump suitability to several applications. P.S.V. has consulted L.G. on the steps of the investigation and the formulation of the concepts and the procedure. P.S.V. has made a thorough refinement of the whole manuscript. J.J.K. has supervised and managed the research actions and the manuscript preparation and finalising, provided consultation to L.G. and P.S.V. on the presentation of the key concepts. T.G.W. has also provided proofreading feedback. All authors have read and agreed to the published version of the manuscript.

**Funding:** This research was funded by the EU project “Sustainable Process Integration Laboratory—SPIL”, project No. CZ.02.1.01/0.0/0.0/15\_003/0000456 funded by EU “CZ Operational Programme Research, Development and Education”, Priority 1: Strengthening capacity for quality research under the collaboration agreement with The University of Waikato, New Zealand.

**Conflicts of Interest:** The authors declare no conflicts of interest. The funders had no role in the design of the study; in the collection, analyses, or interpretation of data; in the writing of the manuscript; or in the decision to publish the results.

## Abbreviations

COP	Coefficient of Performance
CP	Specific Heat Capacity
GCC	Grand Composite Curve
GWP	global warming potential
HEN	Heat Exchanger Network
HP	heat pump
HX	heat exchanger
JCHP	Joule cycle heat pump
MILP	Mixed Integer Linear Programming
MINLP	Mixed Integer Nonlinear Programming
TCHP	transcritical heat pump
T–H	temperature–enthalpy
T–S	temperature–entropy
TSHI	Total Site Heat Integration
VCHP	vapour compression heat pump
VLV	let-down valve

## Nomenclature

$P_2$	The outlet pressure of the compressor in the HP cycle, MPa
$P_5$	The outlet pressure of the expander or expansion valve in the HP cycle, MPa
$Q_h$	Heat output of the heat pump, kW
$R$	The compression ratio of the compressor
$T_5$	The outlet temperature of the expansion valve in the HP cycle, °C
$T_s$	supply temperature
$T_{sink-out}$	The outlet temperature of the sink, °C
$T_t$	Target temperature
$W$	Electrical or power consumption of the heat pump, kW
$\Delta P$	The pressure difference, MPa
$\Delta T$	temperature difference, °C
$\Delta T_1$	The difference between the inlet temperature of the sink and the outlet temperature of the source, °C
$\Delta T_2$	The difference between the outlet temperature of the sink and the inlet temperature of the source, °C
$\Delta T_{in}$	The inlet temperature difference of the source and sink, °C
$\Delta T_{min}$	minimum approach temperature
$\Delta T_{out}$	The outlet temperature difference of the source and sink, °C

## Appendix A

**Table A1.** The stream data of a dairy process. Data from Wallerand et al. [36].

Stream Name	$T_{s_r}$ , °C	$T_{t_r}$ , °C	$\Delta H$ , kW
Refrigeration	6.0	4.0	76.0
Pasteurisation 1a	4.0	66.0	2356.0
Pasteurisation 2a	66.0	86.0	676.4
Pasteurisation 1a	86.0	4.0	2773.2
Pasteurisation 1a	66.0	98.0	119.7
Pasteurisation 1a	98.0	4.0	351.6
Concentration 1	4.0	70.3	504.0
Concentration 2	70.3	70.3	904.2
Concentration 3	66.4	66.4	864.1
Concentration 4	60.8	60.8	849.8
Concentration 5	60.8	4.0	151.5
Concentration 6	68.9	68.9	904.2
Concentration 7	65.9	65.9	864.1
Concentration 9	68.9	15.0	87.8
Concentration 10	65.9	15.0	80.8
Condensates cooling 8	60.1	60.1	849.8
Condensates cooling 11	60.1	15.0	69.7
Yoghurt production 1	4.0	94.0	1026.0
Yoghurt production 2	94.0	10.0	957.6
Desert production 1	4.0	90.0	817.0
Desert production 2	90.0	70.0	190.0
Hot water	15.0	55.0	167.2
Cleaning in place 1a	58.7	70.0	188.6
Cleaning in place 1b	65.0	15.0	104.5
Cleaning in place 2a	67.5	80.0	209.5
Cleaning in place 2b	75.0	15.0	125.4
Fridge	5.0	5.0	300.0

**Table A2.** The stream data of a process of candy processing and packaging. Data from Miah et al. [37].

Stream Name	$T_{s_r}$ , °C	$T_{t_r}$ , °C	$\Delta H$ , kW
Production A			
FP-02	15.0	70.0	13.66
FP-03	15.0	70.0	16.72
FP-04	25.0	60.0	29.12
FP-05	25.0	60.0	29.12
FP-06	30.0	55.0	29.10
FP-07	30.0	55.0	29.10
FP-08	130.0	80.0	60.80
<sup>1</sup> FP-V	120.0	25.0	76.71
FP-08	130.0	80.0	60.80
<sup>1</sup> FP-V	120.0	25.0	76.71
Production B			
15 x S-S	21.0	18.0	279.00
11 x N-S	44.0	47.0	550.00
28 x S-S	44.0	47.0	1400.00
Packaging			
AHU CFP	22	18	55.52

<sup>1</sup> FP-V: Water, includes latent heat.

**Table A3.** The stream data of a 4-column double-effect methanol distillation process. Data from Cui et al. [38].

Stream Name	T <sub>s</sub> , °C	T <sub>t</sub> , °C	ΔH, MW
Crude feed preheated	40.00	85.00	8.160
PC feed preheated	78.94	135.97	13.864
LEC reboiler	78.60	78.62	27.750
PC reboiler	136.10	136.18	114.064
AC reboiler	102.90	102.92	96.267
WC reboiler	102.20	102.22	3.544
First stage condenser	81.76	70.00	26.858
Second stage condenser	70.00	40.00	1.744
PC condenser	130.50	125.19	115.115
AC condenser	66.60	40.00	107.510
WC condenser	66.60	40.00	3.584
PC top stream to tanks	125.19	40.00	7.425

## References

1. Carnot, S. *Reflexions on the Motive Power of Fire: A Critical Edition with the Surviving Scientific Manuscripts*; Manchester University Press: Manchester, UK, 1986; ISBN 978-0-936508-16-0.
2. Radermacher, R.; Hwang, Y. *Vapor Compression Heat Pumps with Refrigerant Mixes*; Taylor & Francis: Boca Raton, FL, USA, 2005; ISBN 978-0-8493-3489-4.
3. Herold, K.E.; Radermacher, R.; Klein, S.A. *Absorption Chillers and Heat Pumps*, 2nd ed.; CRC Press, Taylor & Francis Group: Boca Raton, FL, USA, 2016; ISBN 978-1-4987-1434-1.
4. Lorentzen, G. Trans-Critical Vapour Compression Cycle Device. Patent Application No. WO1990007683A1, 12 July 1990.
5. Pavlas, M.; Stehlik, P.; Oral, J.; Klemeš, J.; Kim, J.-K.; Firth, B. Heat integrated heat pumping for biomass gasification processing. *Appl. Therm. Eng.* **2010**, *30*, 30–35. [[CrossRef](#)]
6. Liew, P.Y.; Walmsley, T.G. Heat pump integration for total site waste heat recovery. *Chem. Eng. Trans.* **2016**, *52*, 817–822.
7. Walmsley, T.G. A Total Site Heat Integration design method for integrated evaporation systems including vapour recompression. *J. Clean. Prod.* **2016**, *136*, 111–118. [[CrossRef](#)]
8. Walmsley, T.G.; Klemeš, J.J.; Walmsley, M.R.W.; Atkins, M.J.; Varbanov, P.S. Innovative hybrid heat pump for dryer process integration. *Chem. Eng. Trans.* **2017**, *57*, 1039–1044.
9. Stampfli, J.A.; Atkins, M.J.; Olsen, D.G.; Wellig, B.; Walmsley, M.R.W.; Neale, J.R. Industrial heat pump integration in non-continuous processes using thermal energy storages as utility a graphical approach. *Chem. Eng. Trans.* **2018**, *70*, 901–906.
10. Stampfli, J.A.; Atkins, M.J.; Olsen, D.G.; Walmsley, M.R.W.; Wellig, B. Practical heat pump and storage integration into non-continuous processes: A hybrid approach utilizing insight based and nonlinear programming techniques. *Energy* **2019**, *182*, 236–253. [[CrossRef](#)]
11. Wang, M.; Deng, C.; Wang, Y.; Feng, X.; Lan, X. Process integration and selection of heat pumps in industrial processes. *Chem. Eng. Trans.* **2018**, *70*, 1105–1110.
12. Urbanucci, L.; Bruno, J.C.; Testi, D. Thermodynamic and economic analysis of the integration of high-temperature heat pumps in trigeneration systems. *Appl. Energy* **2019**, *238*, 516–533. [[CrossRef](#)]
13. Schlosser, F.; Seevers, J.-P.; Peesel, R.-H.; Walmsley, T.G. System efficient integration of standby control and heat pump storage systems in manufacturing processes. *Energy* **2019**, *181*, 395–406. [[CrossRef](#)]
14. Oluleye, G.; Smith, R.; Jobson, M. Modelling and screening heat pump options for the exploitation of low grade waste heat in process sites. *Appl. Energy* **2016**, *169*, 267–286. [[CrossRef](#)]
15. Oluleye, G.; Jiang, N.; Smith, R.; Jobson, M. A novel screening framework for waste heat utilization technologies. *Energy* **2017**, *125*, 367–381. [[CrossRef](#)]
16. Goumba, A.; Chiche, S.; Guo, X.; Colombert, M.; Bonneau, P. Recov'Heat: An estimation tool of urban waste heat recovery potential in sustainable cities. *AIP Conf. Proc.* **2017**, *1814*, 020038. [[CrossRef](#)]

17. Sarbu, I. A review on substitution strategy of non-ecological refrigerants from vapour compression-based refrigeration, air-conditioning and heat pump systems. *Int. J. Refrig.* **2014**, *46*, 123–141. [[CrossRef](#)]
18. Nekså, P.; Rekstad, H.; Zakeri, G.R.; Schiefloe, P.A. CO<sub>2</sub>-heat pump water heater: Characteristics, system design and experimental results. *Int. J. Refrig.* **1998**, *21*, 172–179. [[CrossRef](#)]
19. Nekså, P. CO<sub>2</sub> heat pump systems. *Int. J. Refrig.* **2002**, *25*, 421–427. [[CrossRef](#)]
20. Kim, H.J.; Ahn, J.M.; Cho, S.O.; Cho, K.R. Numerical simulation on scroll expander–compressor unit for CO<sub>2</sub> trans-critical cycles. *Appl. Therm. Eng.* **2008**, *28*, 1654–1661. [[CrossRef](#)]
21. Van de Bor, D.M.; Infante Ferreira, C.A.; Kiss, A.A. Low grade waste heat recovery using heat pumps and power cycles. *Energy* **2015**, *89*, 864–873. [[CrossRef](#)]
22. Fu, C.; Gundersen, T. A Novel Sensible Heat Pump Scheme for Industrial Heat Recovery. *Ind. Eng. Chem. Res.* **2016**, *55*, 967–977. [[CrossRef](#)]
23. Adler, B.; Mauthner, R. Rotation Heat Pump (RHP). In Proceedings of the 12th IEA Heat Pump Conference, Rotterdam, The Netherlands, 15–18 May 2017.
24. Wallerand, A.S.; Kermani, M.; Kantor, I.; Maréchal, F. Optimal heat pump integration in industrial processes. *Appl. Energy* **2018**, *219*, 68–92. [[CrossRef](#)]
25. Linnhoff, B.; Hindmarsh, E. The pinch design method for heat exchanger networks. *Chem. Eng. Sci.* **1983**, *38*, 745–763. [[CrossRef](#)]
26. Gai, L.; Varbanov, P.S.; Walmsley, T.G.; Klemeš, J.J. Process Integration Using a Joule Cycle Heat Pump. *Chem. Eng. Trans.* **2019**, *76*, 415–420.
27. KBC. *Petro-SIM*; KBC Advanced Technologies: London, UK, 2016.
28. Klemeš, J.J.; Varbanov, P.S.; Alwi, S.R.W.; Manan, Z.A. *Sustainable Process Integration and Intensification: Saving Energy, Water and Resources*, 2nd ed.; Walter de Gruyter GmbH: Berlin, Germany, 2018; ISBN 978-3-11-053536-5.
29. Klemeš, J.J.; Varbanov, P.S.; Walmsley, T.G.; Jia, X. New directions in the implementation of Pinch Methodology (PM). *Renew. Sustain. Energy Rev.* **2018**, *98*, 439–468. [[CrossRef](#)]
30. Lopez-Echeverry, J.S.; Reif-Acherman, S.; Araujo-Lopez, E. Peng-Robinson equation of state: 40 years through cubics. *Fluid Phase Equilibria* **2017**, *447*, 39–71. [[CrossRef](#)]
31. Gužda, A.; Szmolke, N. Compressors in Heat Pumps. *Mach. Dyn. Res.* **2015**, *39*, 71–83.
32. Wang, J.F.; Brown, C.; Cleland, D.J. Heat pump heat recovery options for food industry dryers. *Int. J. Refrig.* **2018**, *86*, 48–55. [[CrossRef](#)]
33. Cube, H.L.V.; Steimle, F. *Heat Pump Technology*; Elsevier: Amsterdam, The Netherlands, 2013; ISBN 978-1-4831-0247-4.
34. Klemeš, J.J. *Handbook of Process Integration (PI): Minimisation of Energy and Water Use, Waste and Emissions*; Woodhead Publishing/Elsevier: Cambridge, UK, 2013; ISBN 978-0-85709-725-5.
35. Atkins, M.J.; Walmsley, M.R.W.; Neale, J.R. Integrating heat recovery from milk powder spray dryer exhausts in the dairy industry. *Appl. Therm. Eng.* **2011**, *31*, 2101–2106. [[CrossRef](#)]
36. Wallerand, A.S.; Kermani, M.; Voillat, R.; Kantor, I.; Maréchal, F. Optimal design of solar-assisted industrial processes considering heat pumping: Case study of a dairy. *Renew. Energy* **2018**, *128*, 565–585. [[CrossRef](#)]
37. Miah, J.H.; Griffiths, A.; McNeill, R.; Poonaji, I.; Martin, R.; Leiser, A.; Morse, S.; Yang, A.; Sadhukhan, J. Maximising the recovery of low grade heat: An integrated heat integration framework incorporating heat pump intervention for simple and complex factories. *Appl. Energy* **2015**, *160*, 172–184. [[CrossRef](#)]
38. Cui, C.; Sun, J.; Li, X. A hybrid design combining double-effect thermal integration and heat pump to the methanol distillation process for improving energy efficiency. *Chem. Eng. Process. Process Intensif.* **2017**, *119*, 81–92. [[CrossRef](#)]

